# Dynamic response analysis of a thin-walled rectangular plate subjected to thermoacoustic loadings

**ZHIGAO DANG** *
**ZHAOYONG MAO**

School of Marine Science and Technology, Northwestern Polytechnical University, Xi'an, Shaanxi, 710072, China

**Abstract**   For thin-walled structures invariably exposed to thermal and noise environment, their dynamic response is an extreme concern in the design of the component of advanced hypersonic aircraft. To address the problem, three theoretical models are established with three typical graded thermal distributions considered. By introducing the thermal moment, membrane forces and acoustic loadings into the vibration equation of plate, the governing equation is derived and it is solved combined with boundary conditions of the plate, the modal function and velocity compatibility equations at the fluid-structure coupling surface. The accuracy of the theoretical predictions is checked against finite element results with good agreement achieved. The results show that not the physical parameters with variation of temperature but the thermal moments and membrane forces, cause the buckling phenomenon. It is noted that buckling phenomenon occurs not only in uniform temperature field but also in graded temperature distribution filed. The mechanism analysis about modal snap-through and losing phenomenon indicates that thermoacoustic loadings will affect the stiffness matrix and mass matrix of structure. With the increase of temperature, the lower modes of the plate are lost, the higher modes appear in advance, and the losing phenomenon occurs in accordance with the order.

**Keywords:** Thermoacoustic loadings; Buckling; Dynamic response; Modal snap-through; Rectangular plate

---

*Corresponding Author: Email: zhigao_dang@mail.nwpu.edu.cn

# 1   Introduction

The problem with thermoacoustic environment of thin-walled structures has aroused increasing attention [1–8] since it is subjected to severe environment, which may include mechanical loading, aerodynamic loading, thermal loading and acoustical loading. In the early stage, Blevins *et al.* [9] had investigated thermoacoustic loads and fatigue of hypersonic aircraft skin panels, the thermal and acoustical analysis indicated that the maximum temperature will exceed 1480 °C at the top of the ascent trajectory and the sound levels will exceed 170 dB. As a result, loadings due to engine acoustics and shock impingement dominate the design of many trans-atmospheric aircraft skin panels. Marcus and Otto [10] also mentioned that the aircraft components, such as the inlet, near fuselage and tail, are in a high-temperature and strong-noise environment. These loadings will induce the structures to respond in a nonlinear way, among which the thin-walled structures are likely to snap through under thermoacoustic loadings [11]. This phenomenon is dreadful for the lifetime of the structures, therefore it is necessary to make the structures work in low vibration environment and normal temperature to protect devices in the aircrafts. This work aims to develop a systematic theoretical model to investigate the thermoacoustic dynamic response of a simply supported plate subjected to combination of acoustical and thermal loadings, which could give essential explanation and may provide some guidance for the design of thin-walled aircraft structures.

Lots of literatures have been published to investigate the dynamic performance of structures in thermal loadings. Previous studies by Spain *et al.* [12] had revealed the phenomenon of reduction of natural frequency as the temperature rises. Then, Amit *et al.* [13] studied the modal evolution process exhibited by a curved plate model with clamped-clamped boundary conditions in a high-amplitude random excitation with thermal loading, and they have found that the total system matrix depends heavily on the thermal loading and the average amplitude. They also expected that the frequency of snap-through response need to be further investigated to result in a metric which can be utilized for prediction of fatigue life. Lately, Cheng *et al.* [14] analytically and experimentally investigated high-temperature modal properties, and the results show that the thermal stresses have a much greater effect on the modal characteristics than the change of the material properties due to heating.

As for the dynamic characteristics of plates subjected to compound ther-

moacoustic loadings, its effect on service life of thin-walled plate structure is much more serious than the simple superposition of the single environment. Snap-through phenomenon is easily occurred for plates subjected to compound thermal and acoustic excitations. In 1983, Marcus proposed a simple criteria for the prediction of snap-through phenomenon [15]. Then, NG and Clevenson [16] firstly observed the snap-through phenomenon of thin-walled plate in thermal buckling state, then they proposed statistical response characteristics of thin plate using single degree of freedom model. [17,18] Subsequently, a lot of research on the statistical response of displacement and strain for the single degree of freedom model had been done by Lee [19–21] and Lee *et al.* [22]. As for numerical method, Locke [23] had proposed finite element method (FEM) to solve the structural buckling response of combined thermal and acoustic excitations. With the development of commercial finite element software and thermal noise experiment, the influence of temperature and noise on snap-through phenomenon, the bounds of snap-through phenomenon, and the effect of snap-through of structure on structural fatigue life are gradually investigated [23,24].

Although many of the prior work related to structures subjected to combined thermal and acoustic excitations were concentrated on its vibroacoustic response [1,2], sound transmission performance [3], nonlinear random response [5,6] and fatigue life characteristics [7,8], very few analytical studies have been reported on the further mechanism for dynamic response of plate that would be solved in this paper. To be specific, the natural frequencies and corresponding modal shapes would change under the combination of thermal and acoustic excitations, which is an essential investigation for the following analyses.

The object investigated in this paper is a rectangular titanium alloy plate, and there are many reasons for the material using of titanium alloy over other materials, such as, having a relatively low density, having good resistance to corrosion, having a low thermal expansion coefficient and having growing mechanical properties through heat treatment processes. In the aeronautical industry, many parts are manufactured from titanium alloy, such as frames, engine components including blades, discs, casings and shafts [25]. Due to such characteristics and applications, the research about the dynamic response of titanium alloy plate subjected to thermoacoustic loadings is significant and profound.

In this paper, three analytical models to analyze dynamic response of simply supported isotropic rectangular plates subjected to thermoacoustic

loadings are established, from which the influence of combined three typical graded thermal environments and acoustic excitations on natural frequencies of plates are demonstrated. The layout of this paper is as follows: in Sec. 2, three typical theoretical models are developed for the calculation of natural frequencies under thermoacoustic loadings. Section 3 primarily demonstrates validation of the theoretical model proposed in Sec. 2 and gives an illustrative example only considering physical parameters with the change of temperature, then presents results and discussions for different kinds of thermal field distribution. Finally, conclusions are presented in Sec. 4.

## 2  Analytical model

To mimic the thin-walled plate subjected to thermoacoustic loadings, three rectangular plates are considered to investigate heat transferred from (i) the external to the internal of the fuselage and (ii) one side to the other side of the structure. With reference to Fig. 1, consider a finite, rectangular aeroelastic simply supported plate having length $a$ along $x$-direction, width $b$ along $y$-direction, and thickness $h$ along $z$-direction, subjected to combined acoustical and thermal excitation. The graded temperature environment in thickness direction of the plate is shown in Fig. 1a, with the upper surface of the plate heated by constant temperature $T_1$ and the lower surface maintained at constant temperature $T_2$. Figures 1b and 1c show the graded temperature environment of the plate from one edge to the opposite edge (in width direction of the plate and in length direction of the plate), with one edge of the plate heated by constant temperature $T_1$ and the opposite edge maintained at constant temperature $T_2$. All of the three models are subjected to the external loadings combined acoustical and thermal excitation. The phenomenon of structural buckling, of which the balance configurations of the structure change greatly, would occur where there is a small increment of excitation when the loadings reach a certain value.

As mentioned above, all of the three models with graded temperature environment are governed by Fourier's law of heat conduction, as:

$$\rho C \frac{\partial T}{\partial t} = \kappa \frac{\partial^2 T}{\partial z^2} \ , \ \ \rho C \frac{\partial T}{\partial t} = \kappa \frac{\partial^2 T}{\partial y^2} \ , \ \ \rho C \frac{\partial T}{\partial t} = \kappa \frac{\partial^2 T}{\partial x^2} \ , \tag{1}$$

where $T = T(x, y, z, t)$ is temperature as a function of space and time, $t$ is the time, $x, y, z$ are the Cartesian coordinates, $C$ is the specific heat
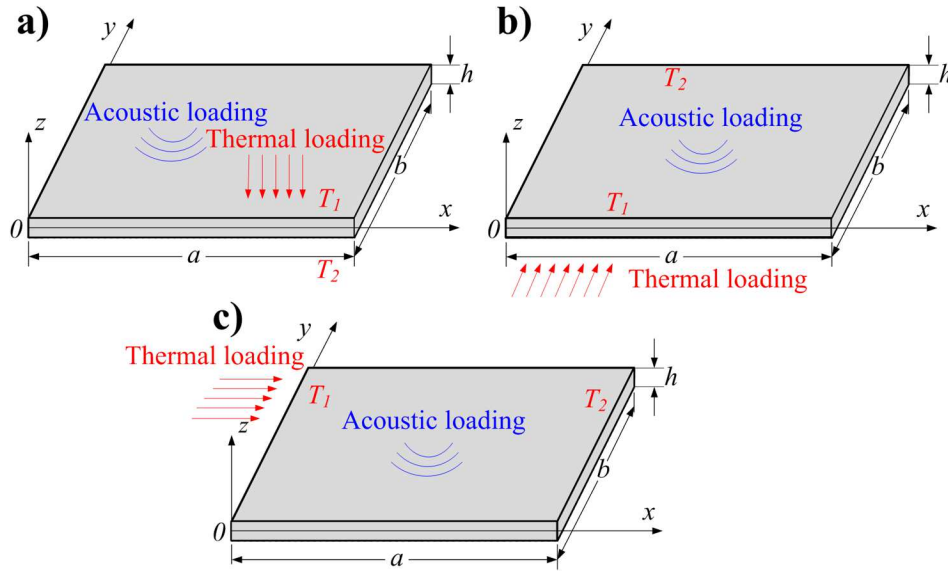
Figure 1: Schematic illustration of a simply supported rectangular plate in acoustical and graded thermal environment: Graded temperature distributed in a) thickness direction, b) width direction and c) length direction.

and $\kappa$ is the thermal conductivity of the plate material, with the thermal boundary conditions specified as:

$$\left\{ \begin{array}{ll} z = \frac{h}{2}, & T = T_1 \\ z = -\frac{h}{2}, & T = T_2 \end{array} \right. ; \left\{ \begin{array}{ll} y = 0, & T = T_1 \\ y = b, & T = T_2 \end{array} \right. ; \left\{ \begin{array}{ll} x = 0, & T = T_1 \\ x = a, & T = T_2 \end{array} \right. . \quad (2)$$

Then Eq. (1) has a solution:

$$T(z) = \frac{T_1 - T_2}{h} z + \frac{T_1 + T_2}{2} ; \quad (3)$$

$$T(y) = \frac{T_2 - T_1}{b} y + T_1; \quad T(x) = \frac{T_2 - T_1}{a} x + T_1 .$$

Considering the similarity of these situations, the detailed calculation process of graded temperature distributed in upper-lower surface direction, shown in Fig. 1a, is presented below.

## 2.1 Critical buckling temperature under thermal loading

Based on von Karman theory for large deflections of thin plate, neutral plane deformation and bending deformation are considered when subjected

to thermoacoustic loading. The membrane force is not only caused by the direct action of neutral plane load, but also related to the deflection of the neutral plane of the plate, which leads to the coupling properties of the bending deformation and membrane stress.

For a simply supported plate, suppose the plane is heated in high temperature fields without acting of other forces, the governing equation can be written as

$$D\nabla^4 w + \rho h \frac{\partial^2 w}{\partial t^2} + \frac{1}{1-\nu} D\nabla^2 M_T = N_{xx}\frac{\partial^2 w}{\partial x^2} + N_{yy}\frac{\partial^2 w}{\partial y^2} + 2N_{xy}\frac{\partial^2 w}{\partial x \partial y} \ , \ (4)$$

where $D$ is the flexural rigidity, $w$ is the transverse displacement, $\rho$ is the density of the plate, $\nu$ is the Poisson's ratio, $M_T$ is the thermal moment given by:

$$M_T = \alpha(T)E(T)\int_{-\frac{h}{2}}^{\frac{h}{2}} T(z)zdz \ , \tag{5}$$

where $\alpha(T)$, and $E(T)$ are the thermal expansion coefficient and Young's modulus as a function of temperature $T$, and $N_{xx}$, $N_{yy}$, and $N_{xy}$ are membrane forces given by

$$\begin{cases} N_{xx} = -\frac{\alpha(T)E(T)}{1-\nu}\int_{-\frac{h}{2}}^{\frac{h}{2}} T(z)dz \\ N_{yy} = -\frac{\alpha(T)E(T)}{1-\nu}\int_{-\frac{h}{2}}^{\frac{h}{2}} T(z)dz \\ N_{xy} = 0 \end{cases} . \tag{6}$$

In uniform temperature field, the thermal moments are zero, thus Eq. (4) can be written as

$$D\nabla^4 w = -\frac{E(T)\alpha(T)h}{1-\nu}\theta\left(\frac{\partial^2 w}{\partial x^2} + \frac{\partial^2 w}{\partial y^2}\right) \ , \tag{7}$$

where $\theta = T(x,y,z,t) - T_{ref}$. Here $T_{ref}$ is the reference temperature before heating.

As shown in Fig. 1a, the plate is constrained by simply supported boundary conditions, requiring:

I The displacement boundary condition: the deformation of the plate edge is zero, the bending moment is zero:

$$x = 0, \ \ a: \ \ w = 0, \ \ \frac{\partial^2 w}{\partial x^2} = 0 \ ; \tag{8a}$$

$$y = 0, \ \ b: \quad w = 0, \quad \frac{\partial^2 w}{\partial y^2} = 0 \ . \tag{8b}$$

II The stress boundary condition:

$$x = 0, \ \ a: \quad N_{yy} = 0, \ \ N_{xx} = 0 \, ; \tag{9a}$$

$$y = 0, \ \ b: \quad N_{yy} = 0, \ \ N_{xx} = 0 \, . \tag{9b}$$

Substituting Eqs. (8) and (9) into Eq. (7), transverse displacement function can be expressed as

$$D \left[ \left( \frac{\pi}{a} \right)^2 + \left( \frac{\pi}{b} \right)^2 \right] = \frac{E(T)\alpha(T)h\theta}{1 - \nu} \ . \tag{10}$$

Then critical buckling temperature can be given by

$$T_s^* = \frac{\pi^2 h^2}{12\alpha b^2 (1 + \nu)} \left( 1 + \frac{b^2}{a^2} \right) \ . \tag{11}$$

## 2.2 Natural frequency under thermoacoustic loading

While considering combined thermal and acoustic excitations, the thermoacoustic governing equation extended from Eq. (4) can be written as

$$D\nabla^4 w + \rho h \frac{\partial^2 w}{\partial t^2} + \frac{1}{1 - \nu} D\nabla^2 M_T$$
$$- \left( N_{xx} \frac{\partial^2 w}{\partial x^2} + N_{yy} \frac{\partial^2 w}{\partial y^2} + 2N_{xy} \frac{\partial^2 w}{\partial x \partial y} \right) = j\omega(\rho_1 \Phi_1 - \rho_2 \Phi_2) \, , \tag{12}$$

where $\omega$ is angular frequency, $j$ is the imaging unit ($\rho_1$, $\rho_2$) are the density of fluid media, ($\Phi_1$, $\Phi_2$) are the acoustic velocity potential in the incident and transmitted field defined as

$$\Phi_1(x, y, z, t) = \sum_{m,n} I_{mn}\varphi_{mn}e^{-j(-k_1 z - \omega t)} + \sum_{m,n} \beta_{mn}\varphi_{mn}e^{-j(-k_1 z - \omega t)} \, , \tag{13}$$

$$\Phi_2(x, y, z, t) = \sum_{m,n} \varepsilon_{mn}\varphi_{mn}e^{-j(-k_2 z - \omega t)} \, , \tag{14}$$

where $I_{mn}$, $\beta_{mn}$, and $\varepsilon_{mn}$ are the $mn$th amplitude of the incident, reflected and transmitted sound, respectively; $\varphi_{mn}$ is the modal function given by

$$\varphi_{mn}(x, y) = \sin \frac{m\pi x}{a} \sin \frac{n\pi y}{b} \ . \tag{15}$$

The local acoustic velocities and sound pressure are related to the velocity potentials by:

$$c_i = -\nabla \Phi_i, \quad p_i = \rho_0 \frac{\partial \Phi_i}{\partial t} = j\omega\rho_0 \Phi_i \quad (i = 1, 2) , \tag{16}$$

where the subscript 0 represents air density.

Consider fluid-structure interaction at the air-panel interface, the following velocity compatibility equations could be obtained to make the normal velocity continuous:

$$-\frac{\partial \Phi_1}{\partial z}\bigg|_{z=\frac{h}{2}} = j\omega w, \quad -\frac{\partial \Phi_2}{\partial z}\bigg|_{z=-\frac{h}{2}} = j\omega w . \tag{17}$$

Substituting Eq. (3) into Eqs. (5) and (6), then the thermal moments and membrane forces can be expressed as:

$$M_T = \frac{(T_1 - T_2)\alpha(T)E(T)h^2}{12} , \tag{18}$$

$$N_{xx} = N_{yy} = -\frac{\alpha(T)E(T)(T_1 + T_2)h}{2(1 - \nu)} . \tag{19}$$

Based on Galerkin principle over the area of the plate, substituting Eqs. (15) and (19) into Eq. (12), there is

$$\iint_s [D\nabla^4 w - \omega^2 \rho h w + \frac{D}{1-\nu}\nabla^2 M_T - 2N_{xx} - j\omega(\rho_1 \Phi_1 - \rho_2 \Phi_2)]\varphi_{mn}(x,y)ds = 0 . \tag{20}$$

Due to the arbitrary $\delta\varphi$, the $mn$th frequency can be written as

$$\omega_{mn} = \left\{ \frac{D}{\rho h} \left[ \left(\frac{m\pi}{a}\right)^2 + \left(\frac{n\pi}{b}\right)^2 \right]^2 + \frac{N_{xx}}{\rho h}\left(\frac{m\pi}{a}\right)^2 + \left(\frac{n\pi}{b}\right)^2 \right.$$

$$\left. -\frac{t_{mn}}{\rho h(1-\nu)}\left(\frac{m\pi}{a}\right)^2 + \left(\frac{n\pi}{b}\right)^2 \right\}^{\frac{1}{2}} , \tag{21}$$

where

$$t_{mn} = 4M_T \frac{[1 - (-1)^m - (-1)^n + (-1)^{m+n}]}{mn\pi^2} . \tag{22}$$

Accordingly, the results of graded temperature distributed in width direction shown in Fig. 1b and in length direction shown in Fig. 1c can be obtained using the similar derivation, which give the relationship between the natural frequency of the plate with simply supported boundary conditions and the different distribution of temperature field.

# 3   Dynamic characteristic analysis and discussion

To determine the dynamic response analysis of a simply supported isotropic rectangular plate under thermoacoustic environment, numerical calculations are carried out to quantify the effects of constant temperature environment and graded temperature environment. The acoustical loading keeps unchanged in different models to investigate the influence of temperature distribution to dynamic characteristics of plates. First of all, the accuracy of model predictions is checked against the numerical results of finite element method (FEM).

## 3.1   Computational comparison between FEM results and analytical results

Since there are few experimental results as reference, to access the accuracy and feasibility of the proposed theoretical model, a FEM numerical model adopting Ansys Workbench 15.0 is developed to calculate the natural frequencies and critical buckling temperature of the plate, whose relevant structural dimensions and physical parameters are listed in Tab. 1. All of the models in Figs. 1a, 1b and 1c are validated, with $T_1 = 1200\,^\circ$C and $T_2 = 20\,^\circ$C. In the numerical model, all the geometrical and physical parameters of the plate are kept the same as those used in the theoretical model. In the numerical calculation, the element type of the plate is shell181, the element type of the air is fluid220, and the fluid-structure interaction coupling is applied to predict the response of the plate subjected to acoustic excitations. The boundary condition of the plate is set as simply supported. The length of each element is less than 1/6 of the acoustic wavelength at the highest frequency of interest to ensure the accuracy of the numerical model [26]. The procedures of finite element analysis are as follows: Firstly, the toolbox of Steady-State Thermal is applied to obtain the total thermal distribution of the plate; then, acoustical response of the plate is achieved by introducing extension of ExtAcoustics_150_42; next, the prestress of the plate is got combined the two loadings above using the toolbox of Static Structural; lastly, the modal analysis is operated. It should be noted that the extension tool of ExtAcoustics_150_42 is a supplement of Ansys Workbench to solve acoustic problems. In the analysis, the extension tool is loaded by clicking on Extensions |Manage Extensions. And then, double-click on Harmonic Response. Different from thermal distribution analysis of the plate, the air domain is added to simulate acoustic

wave transmission in the air. After modeling, setting material properties (titanium alloy and air) for different parts and meshing, the most important step is to define acoustic radiation boundary condition and fluid-structure interaction interface between air and the plate. Finally, the prestress due to acoustic excitations is obtained.

Table 1: Structural dimensions and material properties.

| Elastic plate | |
|---|---|
| Length | $a = 0.6$ m |
| Width | $b = 0.5$ m |
| Thickness | $h = 0.018$ m |
| Young's modulus | $E = 96$ GPa |
| Density | $\rho = 4620$ kg/m$^3$ |
| Poisson ratio | $v = 0.36$ |
| Thermal expansion coefficient | $\alpha = 9.4 \times 10^{-6}$ 1/K |
| Acoustic field | |
| Sound speed | $c_0 = 343$ m/s |
| Density | $\rho_0 = 1.21$ kg/m$^3$ |

Table 2: Comparison of natural frequencies and the first critical buckling temperature.

| Model | Item | $1^{st}$[Hz] | $2^{nd}$[Hz] | $3^{rd}$[Hz] | $4^{th}$[Hz] | $5^{th}$[Hz] | $T_s^*$[°C] |
|---|---|---|---|---|---|---|---|
| 1a | Analytical | 391.46 | 594.45 | 877.52 | 946.54 | 1381.1 | 1117 |
| | FEM | 382.91 | 579.64 | 854.05 | 919.16 | 1341.42 | 1113 |
| | Error [%] | 2.18 | 2.49 | 2.67 | 2.89 | 2.87 | 0.36 |
| 1b | Analytical | 368.43 | 594.69 | 880.34 | 924.51 | 1380.5 | 1079 |
| | FEM | 360.13 | 578.45 | 854.68 | 896.01 | 1335.73 | 1073 |
| | Error [%] | 2.25 | 2.73 | 2.91 | 3.08 | 3.24 | 0.56 |
| 1c | Analytical | 394.23 | 564.5 | 882.18 | 946.39 | 1354.2 | 1025 |
| | FEM | 384.83 | 550.27 | 857.96 | 918.69 | 1312.60 | 1021 |
| | Error [%] | 2.38 | 2.52 | 2.75 | 2.93 | 3.07 | 0.39 |

To validate the proposed theoretical model, Tab. 2 compares the analytical predictions with numerical calculations for the natural frequencies and the first critical buckling temperature. The three proposed typical models, including graded temperature distributed in thickness direction, width direction and length direction of the plate, are all conducted in the computational comparison. The analytical results match well with numerical

results for all the models for natural frequencies of the first five modes and the first critical buckling temperature. The slight difference between the result of FEM numerical model and analytical model may be the result of the ideal boundary handling of the analytical model. To a great extent, the comparisons prove the accuracy and feasibility of the theoretical model, which can then be applied for the following analyses.

## 3.2   Dynamic analysis only considering physical parameters with variation of temperature

There are two possible aspects of thermal loading influencing the modal shape of the structure: (i) the variation of temperature will alter Young's modulus and coefficient of linear expansion of titanium alloy, (ii) the appearance of the thermal loading causes the change of internal mechanical properties of the structure. Both of the two aspects will lead to the change of structural stiffness, which directly affects the natural frequency and modal shape distribution of structures. Therefore, the influence degree of the two aspects is analyzed individually.

In order to evaluate the effect of physical parameters changing with temperature on the modal shape of the plates, modal analysis only considering physical parameters with variation of temperature is carried out in this subsection. The relationships between Young's modulus and coefficient of linear expansion of titanium alloy and temperature are shown in Fig. 2, from which it can be seen that Young's modulus decreases with the increase of temperature, while the change of coefficient of linear expansion is just the opposite. The results of the effect of physical parameters changing with temperature on natural frequency of plates are shown in Tab. 3, the $mn$th order natural frequency of the plate is written as $(m, n)$ in order.

Table 3 demonstrates natural frequency of first five orders only considering physical parameters with the variation of temperature. It can be found that the natural frequency of each order is reduced slightly as a function of temperature. Thus, the preliminary judgement could be drawn that the physical parameters with variation of temperature are not the causes, at least not the main factor, that facilitate the buckling phenomenon. Inevitably, thermal moments and membrane forces are considered to be the main causes for buckling and will be paid more attention to in the following subsections.
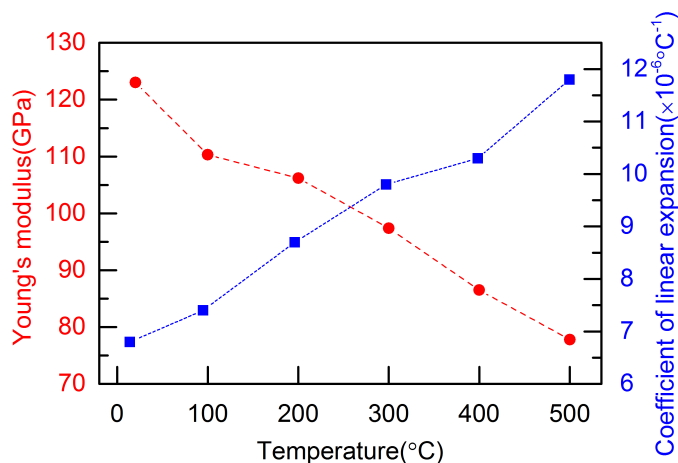
Figure 2:  Young's modulus and coefficient of linear expansion of titanium alloy with the variation of temperature [27].

Table 3:  Natural frequency of first five orders only considering physical parameters with the variation of temperature.

| Order | Frequency [Hz] | | | | | |
|-------|---------|----------|----------|----------|----------|----------|
|       | 20 °C | 100 °C | 200 °C | 300 °C | 400 °C | 500 °C |
| (1,1) | 306.60 | 299.34 | 287.89 | 279.83 | 265.11 | 254.84 |
|       | – | 2.37% | 6.10% | 8.73% | 13.53% | 16.88% |
| (2,1) | 683.56 | 647.31 | 635.16 | 608.28 | 573.23 | 543.64 |
|       | – | 5.30% | 7.08% | 11.01% | 16.14% | 20.47% |
| (1,2) | 849.42 | 808.38 | 793.29 | 758.88 | 716.33 | 681.56 |
|       | – | 4.83% | 6.61% | 10.66% | 15.67% | 19.76% |
| (2,2) | 1226.39 | 1190.35 | 1160.56 | 1120.33 | 1075.45 | 1030.36 |
|       | – | 2.94% | 5.37% | 8.65% | 12.31% | 15.98% |
| (3,1) | 1311.83 | 1290.26 | 1260.96 | 1220.36 | 1180.10 | 1139.31 |
|       | – | 1.64% | 3.88% | 6.97% | 10.04% | 13.15% |

Note:  Each percentage represents the change rate of natural frequency at high temperature (100 °C, 200 °C, 300 °C, 400 °C and 500 °C) compared with the natural frequency at 20 °C for different orders.

## 3.3   Thermoacoustic modal analysis under uniform thermal loading

From the above analysis, it is found that the variation of physical parameter of the structure with changing temperature without considering thermal or

acoustical induced force has no essential influence on natural frequencies. In order to distinguish different factors on natural frequency and modal shape distribution, the influence of thermal moments and membrane forces are considered merely with the physical parameters including Young's modulus and coefficient of linear expansion keeping constant.

When the structure is in a constant uniform temperature field, the thermal moment, $M_T$, in Eq. (5) is zero, while the membrane forces in Eq. (6) are not equal zero. Thus, this subsection gives analysis on dynamic characteristics of structures without considering the thermal moment. Figure 3 shows the variation of the $mn$th natural frequency of the plate with the change of temperature. There are obviously three temperatures, or so 569 °C, 1038 °C, and 1638 °C, at which the phenomena of buckling and snap-through occur. It can be seen from Fig. 3 that the natural frequencies of each order decrease with the increase of temperature before the critical buckling temperature, and the amplitude of reduction is large. When the critical buckling temperature is reached, the plate tends to be unstable, and the natural frequency of (1,1) order is close to zero. At the same time, natural frequency snap-through appears with the increase of temperature. It is noted that the $mn$th natural frequency of the plate decreases with the increase of temperature, and the losing phenomenon occurred in the order of (1,1), (2,1), and (1,2) in the investigated region shown in Fig. 3.
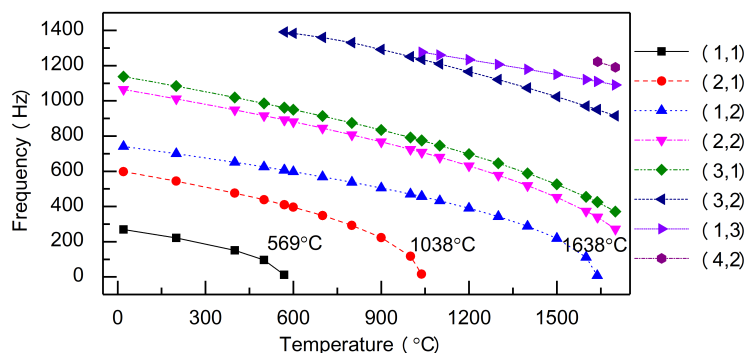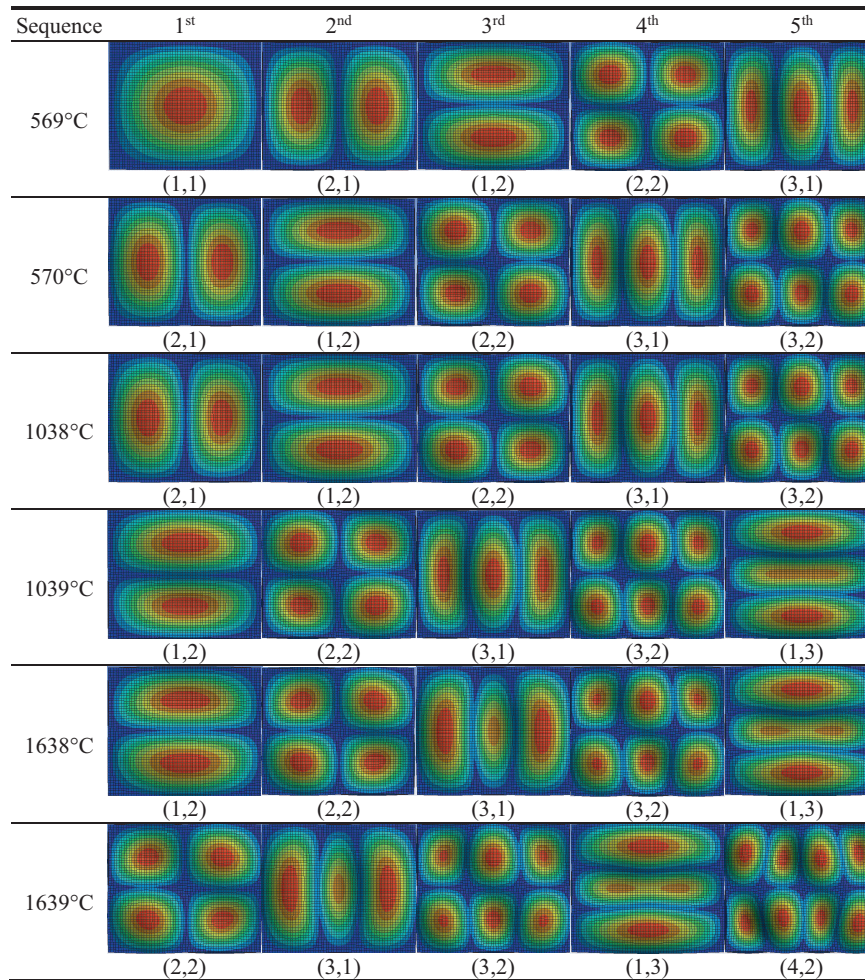


Figure 3: Natural frequency only considering thermal forces induced.

In order to express the change of dynamic characteristics more clearly, the modal shapes of vibration of first five orders under uniform temperature field are shown in Tab. 4. There are six cases of temperature, before and after the three buckling temperatures, are selected. Comparing the modal

Table 4: Modal shape of first five orders under uniform thermal loading.



| Sequence | 1st | 2nd | 3rd | 4th | 5th |
|---|---|---|---|---|---|
| 569°C | (1,1) | (2,1) | (1,2) | (2,2) | (3,1) |
| 570°C | (2,1) | (1,2) | (2,2) | (3,1) | (3,2) |
| 1038°C | (2,1) | (1,2) | (2,2) | (3,1) | (3,2) |
| 1039°C | (1,2) | (2,2) | (3,1) | (3,2) | (1,3) |
| 1638°C | (1,2) | (2,2) | (3,1) | (3,2) | (1,3) |
| 1639°C | (2,2) | (3,1) | (3,2) | (1,3) | (4,2) |

shape at 570 °C with that at 569 °C, the modal shape of (1,1) order is lost, at the same time, the following orders are all moved a position forward. The similar phenomena could be found at 1039 °C and 1639 °C, which are after the second and the third buckling. The modal shape of the $1^{st}$ order at 1639 °C is the $4^{th}$ order at 569 °C or before, and the higher orders are all moved forward, which is in agreement with the results of Fig. 3. With

the increase of temperature, the losing phenomenon of vibration mode is becoming more and more serious. It is remarkable that the loss is not disorderly, but in order from the lower order to the higher order. It is noted that the thermal moments, shown in Eq. (18), equal to zero in uniform thermal environment. Thus, the membrane forces are the most important factors that facilitate the occurrence of buckling in steady temperature field. In order to investigate the loadings with nonzero thermal moments, linear gradient thermal loading combined with acoustic loading are studied in Subsection 3.4.

## 3.4 Thermoacoustic modal analysis under linear gradient thermal loading

Most of the structures subjected to thermoacoustic loadings are under graded temperature distribution, of which the models are presented in this paper. And the previous Subsection 3.3, constant temperature distribution, is just a special case of the theoretical model. There are three subsections: Subsection 3.4.1, Subsection 3.4.2 and Subsection 3.4.3, focused on the temperature gradient in thickness direction, in width direction and in length direction of the plate, of which the diagrammatic sketches are shown in Figs. 1a, 1b, and 1c. In order to investigate thermoacoustic modal under linear gradient thermal loadings, the value of boundary temperatures, $T_1$ and $T_2$, are set firstly, with $T_2 = 20\,^{\circ}\text{C}$. $T_1$ is the higher temperature source shown in $x$-axis in Figs. 4, 5, and 6. Then, the temperature distribution field on the plate is calculated, the result of which combined with acoustic loading are applied to the plate in form of full loadings. With thermoacoustic loadings, the thermal stress field and the acoustic induced stress field of plate are obtained, which provide an essential prerequisite for the further thermoacoustic modal analysis.

### 3.4.1 Temperature gradient in thickness direction of plate

Figure 4 shows the natural frequency of first five orders under linear gradient thermal loading in thickness direction of the plate, from which it can be seen that there is buckling phenomenon when the other boundary temperature is set as $1117\,^{\circ}\text{C}$. The modal shape of first five orders under linear gradient thermal loading in thickness direction of the plate, $20$–$1117\,^{\circ}\text{C}$ and $20$–$1118\,^{\circ}\text{C}$, which are temperature configurations before and after the buckling phenomenon, is shown in Tab. 5.
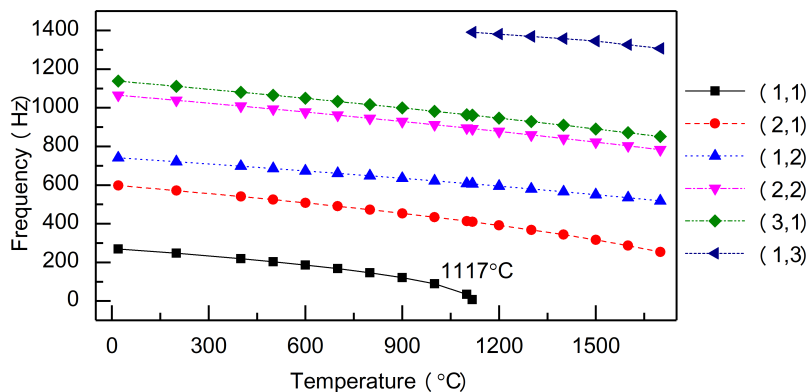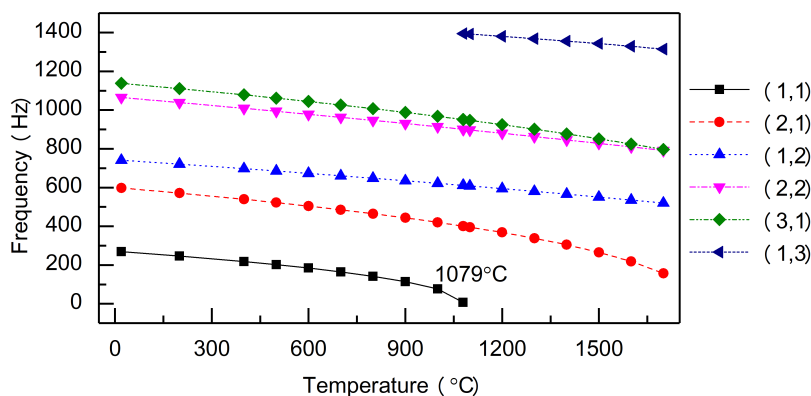
Figure 4: Natural frequency with linear gradient thermal loading in thickness direction of the plate.

Table 5: Modal shape of first five orders under linear gradient thermal loading in thickness direction of the plate.



| Modal Sequence | 1st | 2nd | 3rd | 4th | 5th |
|---|---|---|---|---|---|
| 20°C~1117°C | (1,1) | (2,1) | (1,2) | (2,2) | (3,1) |
| 20°C~1118°C | (2,1) | (1,2) | (2,2) | (3,1) | (1,3) |

It is obvious that the modal shape of first order is lost after buckling and the following orders one step ahead appear, which is in accordance with the results in Subsection 3.3. The losing phenomenon of vibration mode is becoming more and more serious with the increase of temperature $T_1$ under linear gradient thermal loading in thickness direction of the plate. When the structure is in higher temperature environment, the modal shape of the structure has more complicated changes.

### 3.4.2 Temperature gradient in width direction of plate

The natural frequency of first five orders under linear gradient thermal loading in width direction of the plate is shown in Fig. 5. It can be seen that there is buckling phenomenon at about 1079 °C. As a consequence, the temperature configurations, including 20–1079 °C and 20–1080 °C, which are before and after buckling phenomenon, are investigated. Accordingly, the modal shape of first five orders under linear gradient thermal loading in width direction is shown in Tab. 6.



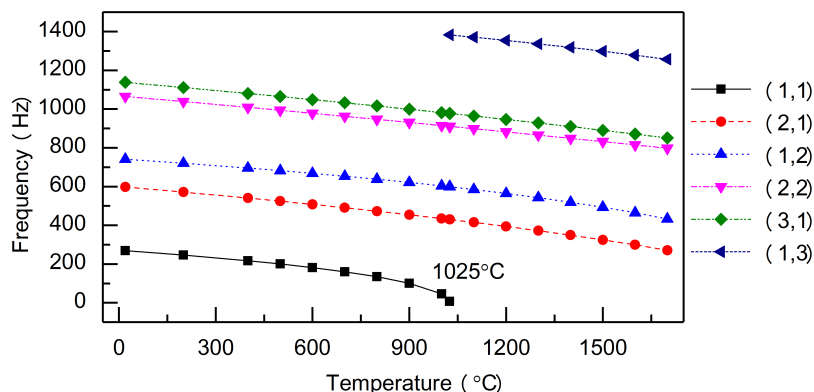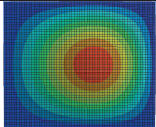Figure 5: Natural frequency with linear gradient thermal loading in width direction of the plate.

Table 6: Modal shape of first five orders under linear gradient thermal loading in width direction of the plate.

| Modal Sequence | 1st | 2nd | 3rd | 4th | 5th |
|---|---|---|---|---|---|
| 20°C~1079°C |  | | | | |
| | (1,1) | (2,1) | (1,2) | (2,2) | (3,1) |
| 20°C~1080°C |  | | | | |
| | (2,1) | (1,2) | (2,2) | (3,1) | (1,3) |

From the results, it is clear that the same losing phenomenon of vibration mode is obtained comparing Tabs. 5, 6, and 7. However, the critical buckling temperature is different in the two situations. Also, it is noticeable that the vibration mode is not symmetric along the direction of linear gradient thermal loading, for example, there are four half-wave in the (2,2) mode shape, where the lower two have larger absolute value at extreme points than the other upper two.

### 3.4.3 Temperature gradient in length direction of plate

Similarly, Fig. 6 shows the variation of the $mn$th natural frequency of the plate with the change of temperature at one side, correspondingly. There are obviously temperature configuration, or so 20–1025 °C, at which the phenomena of buckling and modal snap-through occur. Accordingly, the modal shape of first five orders under linear gradient thermal loading in length direction is shown in Tab. 7.
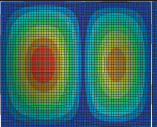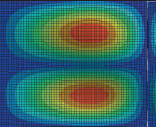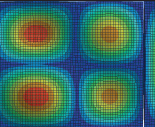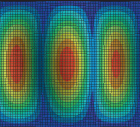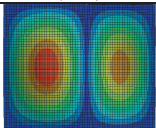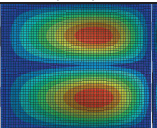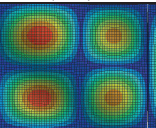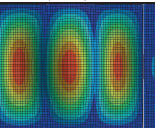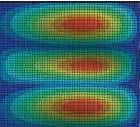


Figure 6: Natural frequency with linear gradient thermal loading in length direction of plate.

It is noticeable that the value of $T_1$ is different when the losing phenomenon of vibration modes happens with $T_2$ keeping at 20 °C. The temperature configurations of thermal gradient in thickness direction, width direction and length direction of the plate are 20–1117 °C, 20–1079 °C, and 20–1025 °C. It is seen that linear gradient thermal loading in length direction is the easiest to happen, while linear gradient thermal loading in thickness direction is the hardest one. As there is no exact solution of critical buckling temperature for structures under nonuniform thermal loading, one possible reason

Table 7: Modal shape of first five orders under linear gradient thermal loading in length
direction of the plate.

| Modal Sequence | 1st | 2nd | 3rd | 4th | 5th |
|---|---|---|---|---|---|
| 20°C~1025°C | | | | | |
| | (1,1) | (2,1) | (1,2) | (2,2) | (3,1) |
| 20°C~1026°C | | | | | |
| | (2,1) | (1,2) | (2,2) | (3,1) | (1,3) |

for explaining the phenomenon is that larger length of linear temperature
distribution leads to earlier appearance of buckling phenomenon.

Also, the asymmetric distribution of vibration mode could also be found
with temperature gradient in length direction of the plate. Taking the mode
shape of (2,2) for an example, the left two have larger absolute value at
extreme points than the other right two of all the four half-wave.

The results in Subsection 3.4 show that the simultaneously existing
thermal moments and membrane forces would induce the occurrence of
structure buckling. Above all, the phenomena of modal snap-through and
losing phenomenon indicate that the modal shape of the plate will be in-
terlaced subjected to thermoacoustic loadings, that is to say, the thermal
loading will lead to the early appearance of a higher order of vibration
mode. The further mechanism is analysed in Subsection 3.5.

## 3.5 Mechanism of modal snap-through and losing phenomenon

The modal snap-through and losing phenomenon mainly occur at structures
with dense modes with very small parameter perturbations. To make it
more clear, the perturbation method is chosen when introducing a small pa-
rameter perturbation of external factors into vibration characteristic equa-
tion by analyzing the changes of eigenvalues before and after perturbation.
Based on the perturbation method, the mechanism of modal snap-through
and losing phenomenon of a simply supported plate mentioned above with

the change of surrounding environments is explicated as follows.

Without considering damping and thermoacoustic loading, the vibration characteristic equation of system can be written as

$$[K_0]\left\{u_0^{(i)}\right\} = \lambda_0^{(i)}[M_0]\left\{u_0^{(i)}\right\} , \tag{23}$$

where $[K_0]$ is the stiffness matrix of structure, $[M_0]$ is the mass matrix of structure, $\lambda_0^{(i)}$ is eigenvalue of $i = 1, 2 \ldots$ mode, $u_0^{(i)}$ is eigenvector with corresponding eigenvalue, subscript 0 represents the original physical properties before imposing thermoacoustic loadings.

When a simply supported isotropic rectangular plate is subjected to thermoacoustic loading, the stiffness matrix and mass matrix of structure will change. After introducing a micro quantity of perturbation, $\varepsilon$, the stiffness matrix and mass matrix of structure can be expressed as

$$[K] = [K_0] + \varepsilon[K_1] , \tag{24}$$

$$[M] = [M_0] + \varepsilon[M_1] , \tag{25}$$

where $\varepsilon[K_1]$ is variation of stiffness matrix, $\varepsilon[M_1]$, is variation of mass matrix, subscript 1 represents the first order perturbation.

Correspondingly, the relevant eigenvalue and eigenvector change with variation of temperature. Then, the expression of eigenvalue and eigenvector are expanded in a power series by using a microquantity of perturbation $\varepsilon$, which can be expressed as:

$$\left\{u^{(i)}\right\} = \left\{u_0^{(i)}\right\} + \varepsilon\left\{u_0^{(i)}\right\} + O(\varepsilon^2) , \tag{26}$$

$$\lambda^{(i)} = \lambda_0^{(i)} + \varepsilon\lambda_1^{(i)} + O(\varepsilon^2) , \tag{27}$$

where $\left\{u^{(i)}\right\}$ and $\varepsilon\lambda_1^{(i)}$ are the first order perturbation of eigenvector and eigenvalue. For simplicity, a higher order of perturbation is not considered in the calculation. Substituting Eqs. (24-27) into Eq. (23) results in

$$[K_0]\left\{u_1^{(i)}\right\} + [K_1]\left\{u_0^{(i)}\right\} = \lambda_0^{(i)}[M_0]\left\{u_1^{(i)}\right\} + \lambda_0^{(i)}[M_1]\left\{u_0^{(i)}\right\} + \lambda_1^{(i)}[M_0]\left\{u_0^{(i)}\right\} \tag{28}$$

According to the expansion theorem, the expansion of $\left\{u_1^{(i)}\right\}$ based on the eigenvector $\left\{u_0^{(s)}\right\}$ of the original system can be expressed as

$$\left\{u_0^{(s)}\right\}^T [K_0]\left\{u_0^{(i)}\right\}^T = \delta_{is}\lambda_0^{(s)} , \tag{29}$$

where $T$ denotes the transpose. Substituting Eq. (29) into Eq. (28), the first order perturbation of eigenvalue can be expressed as

$$\lambda_1^{(i)} = \left\{u_0^{(i)}\right\}^T [K_1] \left\{u_0^{(i)}\right\} - \lambda_0^{(i)} \left\{u_0^{(i)}\right\}^T [M_1] \left\{u_0^{(i)}\right\} . \tag{30}$$

Equation (30) shows that a micro quantity of perturbation has different influence on the eigenvalue of different orders. When two neighboring eigenvalues satisfy the requirement that $\lambda_0^{(i)} \leq \lambda_0^{(i+1)}$, also the first order perturbation meets the requirement that $\varepsilon(\lambda_1^{(i)} - \lambda_1^{(i+1)}) > (\lambda_1^{(i)} - \lambda_1^{(i+1)})$, the result of $\lambda^{(i)} > \lambda^{(i+1)}$ can be obtained. According to the definition of structural dynamics, the modal order is strictly ordered according to the eigenvalues, the eigenvalue of a lower mode would be higher than that of a higher mode when a structural is subjected to perturbation, thus causing the modal snap-through and losing phenomenon.

## 4   Conclusions

In this paper, three theoretical models for the dynamic response of a simply supported rectangular plate subjected to combined thermal and acoustic excitations are developed, and the analytical results are compared with finite element method results. By analyzing the influence of different factors on natural frequency of the structure, the curves of the natural frequency versus temperature are obtained under different conditions of temperature distribution, and the evolution law of modal shapes is investigated in depth. Detailed conclusions can be summarized as follows:

1. Under uniform temperature field, the natural frequency of each order of the plate decreases slightly with the increase of temperature, only considering physical parameters with variation of temperature. And the subsequent analysis indicates that physical parameters of the plate are not a key factor that causes the buckling phenomenon.

2. Neglecting the influence of temperature on material parameters of the plate, and keeping the acoustic loading constant, the influence of membrane forces on natural frequency is considered merely in the dynamic response analysis. The modal snap-through phenomenon at the buckling temperature of 569 °C, 1038 °C, and 1638 °C is observed, before which the natural frequency decreases with the increase of temperature. Then it rises rapidly at the buckling temperature, and decreases again after that.

3. The results of three situations of thermoacoustic modal analysis under linear gradient thermal loadings in thickness direction, width direction and length direction of the plate indicate that the simultaneously existing thermal moments and membrane forces will also cause the buckling phenomenon, which leads to the modal snap-through and losing phenomenon. The mechanism analysis shows that thermoacoustic loadings will affect the stiffness matrix and mass matrix of structure. With the increase of temperature, the lower modes of the plate are lost, the higher modes appear in advance, and the losing phenomenon occurs in order from the lower order to higher order.

The research in this paper is able to demonstrate the change regulation of natural frequency of a simply supported rectangular plate subjected to thermoacoustic loadings, with which the possible reasons for modal snap-through, structural fatigue and destruction are obtained. What is more, it could provide reference for the design of structures, which need vibration protection, such as the thin fuselage structures subjected to simultaneous acoustic and thermal excitations, which need stability avoiding structural resonance to ensure the equipment's normal function, and so forth. Further analysis about the variation of acoustic loading would be conducted then.

*Received 19 October 2018, received in resived form 7 March 2019*

# References

[1] Li X., Yu K., Zhao R.: *Vibro-acoustic response of a clamped rectangular sandwich panel in thermal environment.* Appl. Acoust. **132**(2018), 82–96, DOI: 10.1016/j.apacoust.2017.11.010

[2] Li X., Yu K.: *Vibration and acoustic responses of composite and sandwich panels under thermal environment.* Compos. Struct. **131**(2015), 1, 1040–1049, DOI: 10.1016/j.compstruct.2015.06.037

[3] Li X., Yu K., Zhao R., Han J., Song H.: *Sound transmission loss of composite and sandwich panels in thermal environment.* Compos. Part B-Eng. **133**(2018), 1–14, DOI: 10.1016/j.compositesb.2017.09.023

[4] Kajurek J, Rusowicz A, Grzebielec A: *The influence of stack position and acoustic frequency on the performance of thermoacoustic refrigerator with the standing wave.* Arch. Thermodyn. **38**(2017), 4, 89–107, DOI: 10.1515/aoter-2017-0026

[5] Ibrahim H.H., Tawfik M., Negm H.M.: *Thermoacoustic ramdom response of shape memory alloy hybrid composite plates.* J. Aircraft **45**(2008), 3, 962–970, DOI: 10.2514/1.32843

[6] Ibrahim H.H., Yoo H.H., Lee Y.S.: *Supersonic flutter of functionally graded panels subjected to acoustic and thermal loads.* J. Aircraft **46**(2009), 2, 593–600, DOI: 10.2514/1.39085

[7] Yu W., Wang X., Huang X.: *Dynamic modeling of heat transfer in thermal-acoustic fatigue tests.* Aerosp. Sci. Technol. **71**(2017), 675–684, DOI: 10.1016/j.ast.2017.10.025

[8] Bai W., Sha Y., Li H., Tang X.: *Dynamic response analysis and fatigue life prediction of C/Sic thin laminated plate under thermal-acoustic loadings.* J. Vib. Shock **36**(2017), 10, 76–83, DOI: 10.13465/j.cnki.jvs.2017.10.013

[9] Blevins R.D., Holehouse I., Wentz K.R.: *Thermoacoustic loads and fatigue of hypersonic vehicle skin panels.* J. Aircraft **30**(1993), 6, 971–978, DOI: 10.2514/3.46441

[10] Marcus J.J., Otto F.M.: *Oil canning of metallic panels in thermal-acoustic environments.* In: Proc. 6th Aircraft Design, Flight Test and Operations Meeting, (1974).

[11] Sha Y.D., Wei J., Gao Z.J., Zhong H.J.: *Nonlinear response with snap-through and fatigue life prediction for panels to thermoacoustic loadings.* J. Vib. Control **20**(2014), 5, 679–697, DOI: 10.1177/1077546312463751

[12] Spain C.V., Soistmann D.L., Linville T.W.: *Integration of thermal effects into finite element aero-thermo-elastic analysis with illustrative results.* NASP CR, 1059, 1989.

[13] Amit S., Robert W.G., Joseph J.H.: *Numerical investigation of the snap-through response of a curved, clamped-clamped plate with thermal and random loading.* In: Proc. 49th AIAA/ASME/ASCE/AHS/ASC Structures, Structural Dynamics and Materials Conference, 2008.

[14] Cheng H., Li H., Zhang W., Liu B., Wu Z., Kong F.: *Effects of radiation heating on modal characteristics of panel structures.* J. Spacecraft Rockets **52**(2015), 4, 1228–1235, DOI: 10.2514/1.A33214

[15] Marcus J.J.: *Sonic fatigue of advanced composite panels in thermal environments.* J. Aircraft **20**(1983), 3, 282–288, DOI: 10.2514/3.44865

[16] NG C.F., Clevenson S.A.: *High intensity acoustic tests of a thermally stressed aluminum plate in TAFA.* NASA Tech Memo 101552. NASA Langley R.C. Hampton 1989.

[17] NG C.F., Clevenson S.A.: *High-intensity acoustic tests of a thermally stressed plate.* J. Aircraft **28**(1991), 4, 275–281, DOI: 10.2514/3.46023

[18] NG C.F., Wentz K.: *The prediction and measurement of thermoacoustic response of plate structures.* Proc. 31st AIAA/ASME/ASCE/AHS /ASC Structures, Structural Dynamics and Materials Conf., 1990.

[19] Lee J.: *Large-amplitude plate vibration in an elevated thermal environment.* Appl. Mech. Rev. **46**(1993), 2, 242–254, DOI: 10.1115/1.3122643

[20] Lee J.: *Random vibration of thermally buckled plates: II Nonzero temperature gradient across the plate thickness.* Appl. Mech. Rev. **50**(1997), 2, 105–116, DOI: 10.1115/1.3101821

[21] LEE J.: *Displacement and strain statistics of thermally buckled plates.* J. Aircraft **38**(2001), 1, 104–110, DOI: 10.2514/2.2740.

[22] LEE J., WENTZ K., CLAY C., ANSELMO E., CRUMBACHER R., VAICAITIS R.: *Prediction of statistical dynamics of thermally buckled composite panels.* In: Proc. 39th AIAA/ASME/ASCE/AHS/ASC Structures, Structural Dynamics and Materials Conf., 1998.

[23] LOCKE J.: *Finite element large deflection random response of thermally buckled plates.* J. Sound Vib. **160**(1993), 301–312, DOI: 10.1006/jsvi.1993.1025

[24] GOLEY G., ZAPPIA B., BEBERNISS T., SHUKLA A.: *Effect of loading on the snap-through response of a post-buckled beam.* In: Proc. 49th AIAA/ASME/ASCE/AHS/ASC Structures, Structural Dynamics, and Materials Conf., 2008.

[25] BRAN D.T., ELEFTERIE C.F., GHIBAN B.: *Aeronautical industry requirements for titanium alloys.* IOP Conf. Ser.: Mater. Sci. Eng. **209**(2017), 1, 012059, DOI: 10.1088/1757-899X/209/1/012059

[26] HOWARD C.Q., CAZZOLATO B.S.: *Acoustic analyses using Matlab and Ansys.* CRC Press, 2014.

[27] LI J.Y.: *Thermal acoustic fatigue analysis of flight vehicle thin-walled structures.* MSc thesis, Shenyang Aerospace University, Shenyang 2011.